Biological Procedures Online

RESEARCH

Open Access

Leishmania Infection: A Bioorganic Model Under the *Light* of Benchtop Low Field Nuclear Magnetic Resonance

Jairo Mendoza-Roldan[1†], Paola Albanese[3,4†], Carmela Di Spiridione[2], Mirco Vacca[2], Matteo Spagnuolo[2], Mario Alves[1], Mariaelisa Carbonara[1], Maria De Angelis[2], Danilo Vona[2*] and Domenico Otranto[1,5]

Abstract

Background Low-field benchtop Nuclear Magnetic Resonance (NMR) spectrometers rely on permanent magnets and do not require deuterated solvents, being increasingly employed for quality control and the profilometric assays of complex matrices from food products to metabolically enriched exudates. In this study, the non-destructive, non-invasive, low-cost and time-effective nature of benchtop NMR investigations was exploited to separate Leishmania infantum -positive and -negative dog (Canis lupus familiaris) sera. Moreover, among the Leishmania-positive samples, sera with either circulating free or complexed antibody molecules displayed distinctive NMR profiles with promising discriminatory potential.

Methods This approach is made possible by the identification of specific bioorganic 1D and 2D NMR signals, such as protons found in pyranose (PYR), phospholipid (SPC), and acetyl moieties (Glyc), whose distribution in serum samples varies in association with specific parasitic infections.

Results The discrimination among Leishmania Negative (n=5) vs Low positive (n=8) samples was successfully performed using the summed integration areas of 3 main buckets (SPC, Glyc, late PYR), while the analytical speciation of High (Ab+) positive (n=8) samples was reached recurring to a further integrated area, belonging to early PYR signals.

Conclusion The characterization of inflammatory states through traces of oxidized lipids, and the study of immunological activation using bioorganic signals of glycoproteins, can be easily exploited on a broad scale even in different pathological contexts with features similar to the Leishmania case report.

Keywords Bioorganic Traces, Low Field NMR, *Leishmania*, Benchtop Technology

†Jairo Mendoza-Roldan and Paola Albanese contributed equally as first names.

*Correspondence:
Danilo Vona
danilo.vona@uniba.it
[1]Dipartimento di Medicina Veterinaria, Università Degli Studi di Bari "Aldo Moro", Valenzano, Bari 70010, Italy
[2]Dipartimento di Scienze del Suolo, della Pianta e degli Alimenti (Di.S.S.P.A.), Università Degli Studi di Bari "Aldo Moro", Bari, Italy
[3]Dipartimento di Scienze Fisiche, della Terra e dell'Ambiente, Università degli Studi di Siena, Siena 53100, Italy
[4]Dipartimento di Biotecnologie, Chimica e Farmacia, Università degli Studi di Siena, Siena 53100, Italy
[5]Department of Veterinary Clinical Sciences, Jockey Club College of Veterinary Medicine and Life Sciences, City University of Hong Kong, Kowloon, Hong Kong, China

© The Author(s) 2026. **Open Access** This article is licensed under a Creative Commons Attribution-NonCommercial-NoDerivatives 4.0 International License, which permits any non-commercial use, sharing, distribution and reproduction in any medium or format, as long as you give appropriate credit to the original author(s) and the source, provide a link to the Creative Commons licence, and indicate if you modified the licensed material. You do not have permission under this licence to share adapted material derived from this article or parts of it. The images or other third party material in this article are included in the article's Creative Commons licence, unless indicated otherwise in a credit line to the material. If material is not included in the article's Creative Commons licence and your intended use is not permitted by statutory regulation or exceeds the permitted use, you will need to obtain permission directly from the copyright holder. To view a copy of this licence, visit http://creativecommons.org/licenses/by-nc-nd/4.0/.

Introduction

Early detection of an immune-mediated disease may be achieved through unconventional benchtop spectroscopic techniques capable of probing biological samples at a purely molecular level. Among these, pre-metabolomic nuclear magnetic resonance (NMR) investigations represent a promising approach [1]. Low-field benchtop NMR is widely employed for metabolomic pre-screening of complex biological samples, comprising serum, urine and exudates. Given its affordability, ease of use and portability, benchtop NMR enables the correlation of complex chemical information with pathophysiological conditions, supporting both research applications and clinical assessment or follow-up. Additionally, benchtop NMR may be effortlessly used to identify metabolic biomarkers, diagnose diseases, and monitor treatment response. Indeed, recent research has successfully applied high-field NMR-based methodology for serum lipoprotein profiling to routine benchtop systems, rendering these techniques particularly valuable [2, 3]. This new application is based on the well-established relation between the composition and abundance of circulating supramolecular lipids and proteins assemblies with cardiovascular and chronic inflammatory states.

Among the macromolecular features detectable through NMR spectra, serum exhibits characteristic acetyl resonances originating from O- and N-acetylated carbohydrates, associated with modified protein backbones. Specifically, circulating glycoproteins operate at the interface of signaling and structural regulation, functioning as messengers (e.g., interleukins), carriers, and key mediators of the immune response (i.e. acute-phase proteins and antibodies). Consequently, the emergence of these acetyl resonances has previously been associated with acute-phase proteins produced in response to a wide range of dysfunctions or dysmetabolic conditions [4]. These signals, located around 2 ppm (GLYC), correspond to α-methyl groups in N-acetylglucosamine and N-acetylgalactosamine moieties, as well as N-acetyl methyl groups of neuraminic (or sialic) acid [5]. It is widely accepted that these H-methyl resonances arise from α-1-acid glycoprotein, haptoglobin, serotransferrin, α-1-antitrypsin, α-1-antichymotrypsin, selected interleukins and immunoglobulins (i.e., antibodies of the IgG and IgM classes) in most of mammalian serum samples, with few exceptions.

A secondary, minor yet biologically significant signal appears around 3.2 ppm, corresponding to the SPC bucket. SPC is part of the inflammatory signature and its resonance originates from the methyl groups (-CH_3 coupling) of trimethylammonium moieties, belonging to the choline headgroup of protein-linked phospholipids [6]. In serum, these supramolecular assemblies predominantly constitute high- and low-density lipoprotein particles (HDL and LDL), which play an essential role in lipid and metabolite transport [2]. Their spectral signatures are frequently altered under various pathological conditions. The SPC region specifically reflects the -CH_3 coupling with trimethylammonium-bearing phospholipids within lipoprotein complexes, and its integrated intensity strongly correlates with inflammatory activation, oxidative stress and early, broadly reactive host-defense response [6].

Importantly, the predictive value of NMR-derived information from these biomacromolecular regions is well established in metabolic disorders, including obesity and insulin resistance [7]. In addition, NMR datasets have also been correlated with infectious disease states, supported by the extensive availability of serum samples from COVID-19 biobank [8].

Despite the abundance of glycoprotein signals contributing to the GLYC region, only a limited number of studies [4] have been effectively exploited to determine which acute-phase proteins most strongly influence the overall GLYC trace in serum NMR profiles. However, thus far, this technique has not been applied for parasitic immune-mediated diseases such as in the case of leishmaniases. Yet, this approach could be useful also in veterinary medicine as it is grounded in the well-established notion that the domestic dog (*Canis lupus familiaris*) is a widely investigated model organism from a metabolomic standpoint.

Importantly, dogs represent the main reservoir of *Leishmania infantum*, and in endemic areas they are the primary blood source for sand fly vectors. This protozoan is the causative agent of zoonotic canine leishmaniosis (CanL) across many tropical and subtropical regions, including the Mediterranean basin [9]. The pathogenesis of CanL is driven by the delicate immunological balance established between the intracellular amastigote stage of the parasite and the host immune system, with disease progression varying according to the prevailing immune response. Indeed, a predominant Th1 cellular response tends to limit the parasite load, hence being protective, whereas a Th2-skewed humoral response is detrimental, leading to the increased expression of anti-inflammatory cytokines that favor the formation of soluble circulating immune complexes (sCIC). These complexes have a pivotal role in the clinical onset as they eventually may precipitate and deposit in the endothelium of different organs. Importantly, the clinical discrimination between an infected yet clinically healthy dog and one progressing towards disease depends on these immunological fluctuations [10]. To date, only an ELISA-based diagnostic tool has been standardized to isolate and quantify sCIC for dogs with CanL. However, there is not a method that can rapidly identify sCIC, having a predictive value on their

formation and concentration that may allow early staging and treatment of the disease [11].

Conversely, NMR analysis may be well suited for profiling canine serum because species-specific differences in the O- and N-glycosylation profiles concern mainly the relative abundance of certain sugars rather than the structure or chemical composition of acetyl-bearing moieties. For instance, galactosylated and sialylated glycans are less abundant in dogs, while trace acetylation remains adequately distributed [12]. Furthermore, correlating the GLYC signal with antibody abundance is particularly straightforward in this species, as IgG constitutes the most abundant serum glycoprotein. Nevertheless, NMR-based metabolic profiling in dogs remains markedly underrepresented in the literature. Thus, the present study aimed to employ benchtop, low-field, rapid, non-invasive, and non-destructive NMR technology to evaluate the feasibility of correlating specific NMR integration buckets in serum of dogs infected by *L. infantum*.

Materials and Methods

Bidistilled water, α1-acid glycoprotein purified from plasma (GP), from cow source (cGP), α1-antitrypsin purified from plasma (AT), dog antibody purified from plasma (Ab), albumin protein (Alb), macromolecular Ab complex from pig (mAb), D-(+)-glucose, N-acetyl-D-mannosamine, N-acetylneuraminic acid, N-acetyl-D-glucosamine, N-acetyl-D-galactosamine were purchased from Merck-Sigma Aldrich. Canine serum samples were collected as described below.

General Information on Dog Sera Collections

Dog blood samples (n = 21), collected as part of a previous study [13], were obtained from the cephalic vein and placed into tubes without anticoagulant to allow clot formation. After centrifugation (15 min at 1500 x g) serum was collected for a complete biochemical panel including acute phase proteins (i.e., CRP) and ferritin, serum capillary electrophoresis, and serology. Serum samples were analyzed for *L. infantum* antibodies by IFAT as previously described [14] and considered positive if clear cytoplasmic and membrane fluorescence of *L. infantum* promastigotes from a cut-off dilution of 1:80 was evident. Positive sera were titrated by serial two-fold dilutions (i.e., 1:80, 1:160, 1:320, 1:640, 1:1280) up to 1:5120. Samples were considered negative if they failed to produce a positive result at 1:80. Serum samples from a dog positive for *L. infantum* by cytological and molecular analyses, and a healthy dog negative for *L. infantum*, were used as positive and negative controls, respectively. In addition, serum samples were tested for anti-*L. infantum* antibodies using a commercial enzyme-linked immunosorbent assay (ELISA) (VetLine Leishmania ELISA, Novatec Immunodiagnostica GmbH, Germany). Genomic DNA (gDNA) was extracted from blood, using a commercial GenUP Blood DNA kit (Biotechrabbit GmbH, Hennigsdorf, Germany), according to the manufacturer's instructions. All samples were tested for *L. infantum* kDNA minicircle (120 bp) by real-time PCR (qPCR), using the protocol described elsewhere [15]. Dogs were divided into three groups: negative, low positive and high positive for *L. infantum.*

One-dimensional ^{1}H-NMR

^{1}H NMR experiments on dog sera (600 µL per animal) were performed on a Spinsolve 80 H/C Ultra benchtop low field NMR spectrometer (Magritek) at a ^{1}H Larmor frequency of 80 MHz. All the experiments were conducted after preparing a fresh stock of formic acid in water (FA solution, stock concentration: 2.2 mM) here chosen as a high δ standard molecule for analytical reference and mixing 0.2 mL of FA with 0.6 mL of each serum sample. The acquisition was done using the following parameters: WET suppression mode (Water suppression Enhanced through T1 effects, 5.2–4.4 ppm range), 4 dummy scans, 16 scans, 0.94–0.98 correction factor, deactivated C decoupling function, exponential apodization (0.1). All spectra were phase and baseline corrected, and the spectral alignment was done on solvent signal (δ water: 4.79 ppm). Frequent shimming programs were set with a D_2O: H_2O 1:10 solution. Time for the single spectrum acquisition: 4.2 min. Experimental temperature was monitored, and resulted constant at 20 ± 0.2 °C.

The semi-quantitative NMR (relative comparison of protons belonging to different moieties) outputs are directly calculated from the NMR peak integrals of each bucket area over FA reference, using the following formula:

Total ^{1}H Signals:

$$\sum_{i=1}^{N} Asi$$

with:

A_{si}: Integral of the area belonging to the analyte signals (normalized on FA reference).

Note: in case of Leishmania(+) vs. Leishmania(-), summed areas (N) belong to SPC, Glyc and Late Pyr; in case of Leishmania(+, Ab+) vs. Leishmania(+,Ab-), summed areas (N) belong to SPC, Glyc, early Pyr and Late Pyr.

Recording of D-glucose in water was performed to verify possible overlapping coming from blood sugar content towards SPC or GLYC areas (Figure S1) [16].

Formic acid (FA), as internal molecular reference, has been compared to other 3 reference molecules (catechol, acetic acid, benzoic acid), and lipid signals (1.05–0.63

ppm) in 3 blood sera samples have been integrated over all these molecular references. This reference control underlined a good robustness in the use of FA during the experimental processings.

Two-dimensional ^{1}H-^{1}H 2D-COSY

^{1}H-^{1}H 2D-COSY experiment was recorded with the pulse sequence at 90°, passing from 256 increments in the indirect dimension with 13 ppm bandwidth, 4 scans of acquisition per increment, 2 dummy scans, apodization along T1 (first point 0.5), sine bell 0 deg for F2. Time for the single spectrum acquisition: 16.2–18.2 min. Experimental temperature was monitored, and resulted constant at 20 ± 0.2 °C.

Two-dimensional ^{1}H-^{13}C 2D-HSQC

^{1}H-^{13}C 2D-HSQC experiment was recorded with 32 scans, 1 sec repetition time, with f1 bandwidth of 170 ppm, and 128 increments. apodization along T1 (first point 0.6), sine bell 0 deg for F2. Time for the single spectrum acquisition: 36.2–38.4 min. Experimental temperature was monitored, and resulted constant at 20 ± 0.2 °C.

Statistical Validation

Multivariate correlative analysis for clustering of data has been performed using the free tool online available, including Principal Component Analysis Calculator online, from Statistic Kingdom applications toolset, Biological Magnetic Resonance Bank in metabolomics (BMRB) and MetaboAnalyst. Data have been analyzed after autoscaling system [17]. Data have been analyzed after autoscaling system, with a mean-centering for each metabolite across all samples divided over standard deviation. The heatmap was generated in MetaboAnalyst using autoscaled data. Sample clustering was performed using Euclidean distance and Ward's linkage method. NMR buckets included in the heatmap were ranked and filtered based on univariate t-test results, applying a significance threshold of $p < 0.05$.

Table 1 Groups of dogs (Negative, low positive, high positive) included in the study depending on the IFAT, qPCR (positivity expressed in cycle threshold – *ct*), and ELISA for *Leishmania infantum*

Group	Dog ID	IFAT L. infantum	qPCR	ELISA
Negative (*n* = 5)	1–5	-	-	-
Low positive (*n* = 8)	6	1:80	-	-
	7	1:640	-	-
	8	1:640	-	-
	9	1:80	-	-
	10	1:640	Positive (*ct* 36.2)	-
	11	1:80	-	-
	12	1:160	-	-
	13	1:320	-	-
High positive (*n* = 8)	14	1:5120	Positive (*ct* 32.5)	Positive
	15	1:1280	-	-
	16	1:2560	Positive (*ct* 32.4)	Positive
	17	1:2560	Positive (*ct* 30.4)	Positive
	18	1:1280	-	-
	19	1:2560	Positive (*ct* 18)	-
	20	1:2560	Positive (*ct* 29)	Positive
	21	1:1280	Positive (*ct* 28)	-

Results

Characterization of *Leishmania Infantum* Infection in Dog Groups

Animal groups were composed by negative control ($n = 5$) or eight animals either low- or high-positive individuals. The negative control group were apparently healthy animals, negative for serological and molecular screening, without biochemical alterations or clinical signs of CanL (Table 1). The low-positive group consisted on animals with IFAT antibody titers from 1:80 to 1:640. Of this group, one animal had positivity to qPCR for *L. infantum* and IFAT positivity of 1:640, and none of the animals were positive to ELISA. In addition, *L. infantum* high positive group included seropositive animals (i.e., IFAT antibody titers from 1:1280 to 1:5120) with 4 animals being also positive in ELISA and 6 at qPCR (Table 1).

One-dimensional ^{1}H-NMR of Dog Serum and Positive vs. Negative Correlative Study

Recording a one-dimensional NMR spectrum of canine blood sera led to the isolation of 12 bucket signals (b1-b12, Fig. 1, Table S1), which were integrated using an internal reference (*H*-COOH, FA, 8.47 ppm in water), and subsequently correlated *via* software. All the buckets so gave an integral area over FA reference, and these values were compared among samples. Across the analyzed samples, this approach enabled the definition of a multivariate threshold that differentiated *Leishmania*-positive from *Leishmania*-negative cases. Statistical mapping analysis (heat map of all bucket areas, Figure S2a) highlighted 5 bucket regions with consistent discriminatory patterns, thus providing clear separation between *Leishmania* negative vs. positive samples. This initial statistical screening allowed the selection of specific areas of investigation. Among the 12 buckets, the regions showing the strongest correlation with *Leishmania* positivity (cf., r^2: 88.9%) were following integrative zones: 4.30–3.86 (cy(ring)pyranose, namely late pyranose, PYR), 3.31–3.06 (H_3-C in trimethylammonium from free choline residue in phospholipids, SPC), 2.18–2.09 (H_3C-C = O N-acetyl, late glycosylation GLYC) 2.11–1.98 (H_3C-C = O N-acetyl, O-acetyl, late glycosylation site, GLYC), 1.98–1.80 (H_3C-C = O N-acetyl, O-acetyl, early glycosylation site, GLYC) ppm (Fig. 2b).

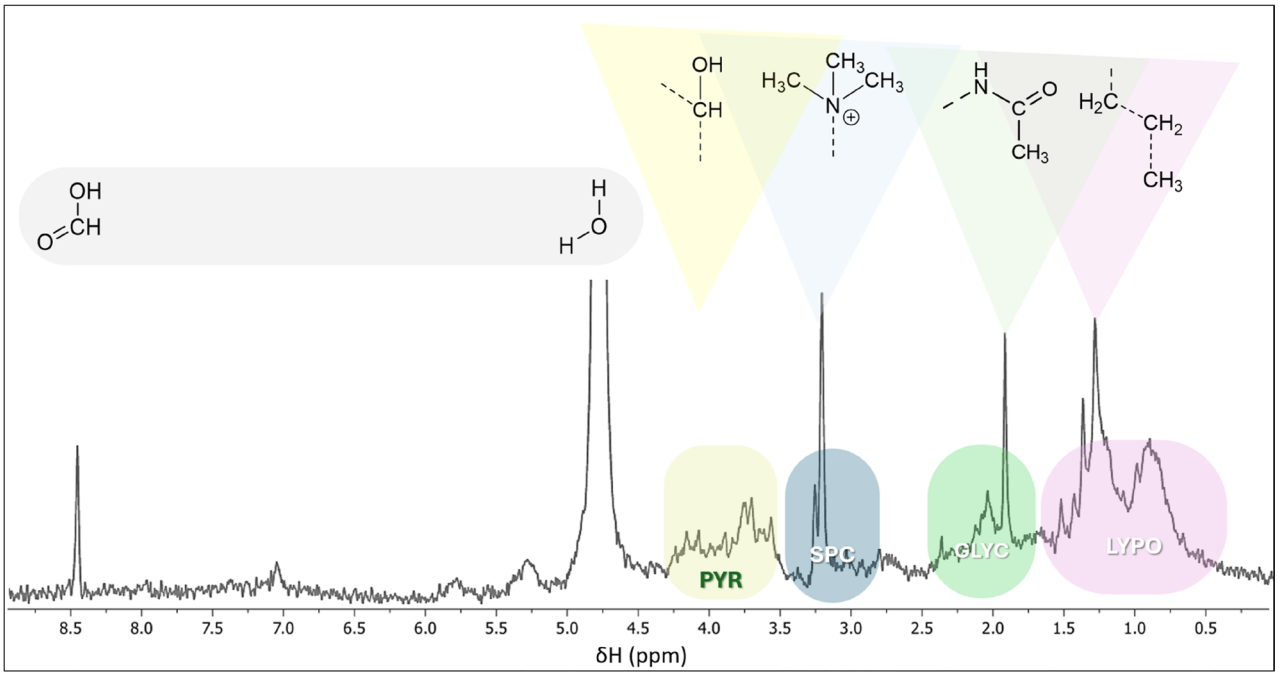


Fig. 1 Chemical shift peaks attribution to macromolecular bucket signals in dog unpurified blood serum, using H_2O as solvent and formic acid as internal molecular reference (80 MHz, Table S1 in Supporting Information Section)

Except for the SPC area, all discriminating bucket areas were correlated to pyranose ring or α-methyl in N-/O-acetyl sugar prosthetic chemical groups linked to serum glycoproteins. Separation accuracy further improved when cumulative data for SPC, GLYC and late PYR zones (expressed as summed normalized integrated areas) were evaluated as illustrated by the box-histograms distribution (Fig. 3a). As also indicated by the VIP plot, the SPC region contributed most strongly to the discrimination of *L. infantum* positive sera, likely reflecting an early, non-specific inflammatory activation, not necessarily associated with antibody production(Figure S2b).

Chemical Speciation of GLYC Zone via Bidimensional NMR-based Deconvolution

To better understand the nature of the GLYC signals, particularly in relation to *Leishmania*-positive sera with low- versus high-antibody titers (i.e., low-positive vs. high-positive groups), we acquired both.

^{1}H-^{1}H-COSY and ^{1}H-^{13}C-HSQC spectra to examine the signals around 2 ppm in canine serum samples. The Proton-proton homo-correlated analysis (Fig. 3a) revealed increased signal complexity within the GLYC region of Antibody-enriched positive sera; however, proton-proton contour maps did not show robust resolution and speciation of glycoprotein acetyl signals. Table S2 reports H signal ranges for the specific GLYC regions investigated for macromolecular standard.

Conversely, the ^{1}H-^{13}C-HSQC (Fig. 3b) [18] provided clearer structural definition, revealing three superimposed sets of signals between 1.90 and 2.15 ppm in the ^{1}H-dimension, each exhibiting strong frequency correlation across distinct ranges in the ^{13}C-dimension: (i) signals of protein methionine ε-methyl groups (15–19 ppm), (ii) N-acetyl methyl groups of glycans Glyc (20–27 ppm), (iii) and lipidic allyl groups in yellow (27–35 ppm).

Considering the high selectivity within the combined ^{1}H Glyc-^{13}C Glyc region (Pink zone correlation), and the population of Glyc antibody-based molecular signal assigned in (^{1}H)1.92–2.2 ppm: (^{13}C) 21.5–25 ppm correlation area, this experiment allowed a selective detection of specific contour map related to the presence of abundant Ab concentrations especially in *Leishmania*-positive and Ab-enriched dog sera (See attributions of standard molecules: Figure S4).

Correlative Study for High- vs. Low- Antibodies in *Leishmania* Positive Sera

Statistical mapping analysis was also applied to differentiate two populations within the *Leishmania*-positive cohort characterized by high (Ab^{+}) or by low (Ab^{-}) levels of CICs. In Fig. 4a an initial correlative analysis was performed by including both the late and the early PYR area, corresponding to the multiple cy(ring)pyranose peak (i.e., 3.86–3.46 ppm range), as an additional bucket (currently summed to late PYR for the correlative heatplot study). This strategy yielded a clear separation between Ab^{-} and Ab^{+} samples, improving the confidence value (> 90.9%).

As observed in the previous comparison, separation between Ab^{-} and Ab^{+} samples further improved when

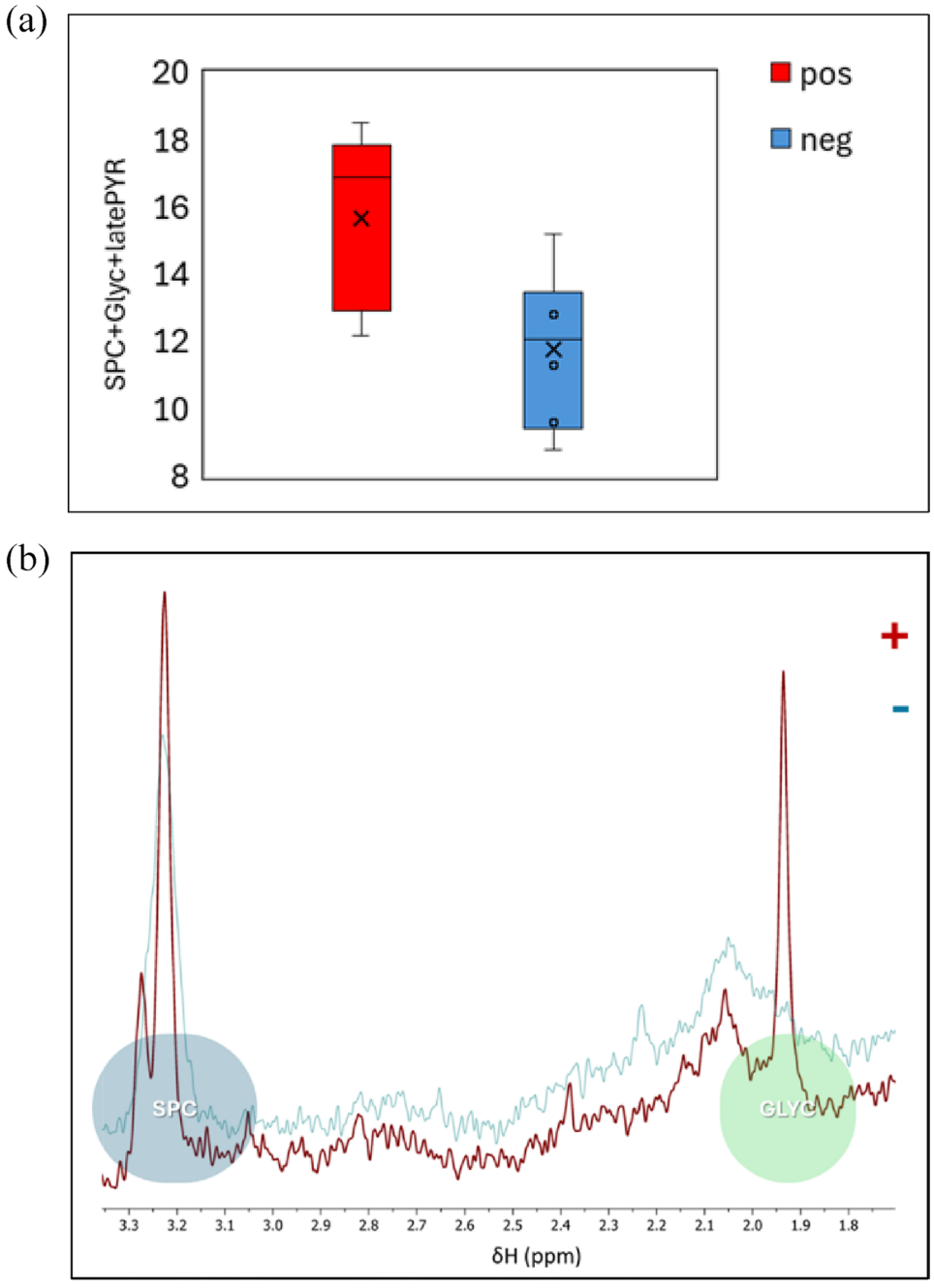


Fig. 2 **a** Box-histograms distribution of cumulative data for SPC, Glyc and late PYR zones (*Total*^{1}*H Signals*); **b** spectroscopic differences between positive and negative blood sera (focus)

cumulative data from SPC, GLYC and total PYR zones (expressed as summed normalized integrated areas) were considered, as illustrated in Fig. 4b. Conversely, the VIP plot for these three regions indicated that GLYC was the most significant and discriminative NMR bucket, whereas SPC played a minor role (Figure S3). This outcome is expected as circulating antibody concentrations increase in canine serum, the resulting spectral features become more strongly associated with glycoprotein-rich components and less inflammatory (phospholipid-related) signals.

Discussion

Results from the present study highlighted the usefulness of a benchtop low field NMR for discriminating *L. infantum* infection in dogs. Moreover, despite the low specificity of the NMR technology, the average sensitivity and low-field, rapid, non-invasive, and non-destructive

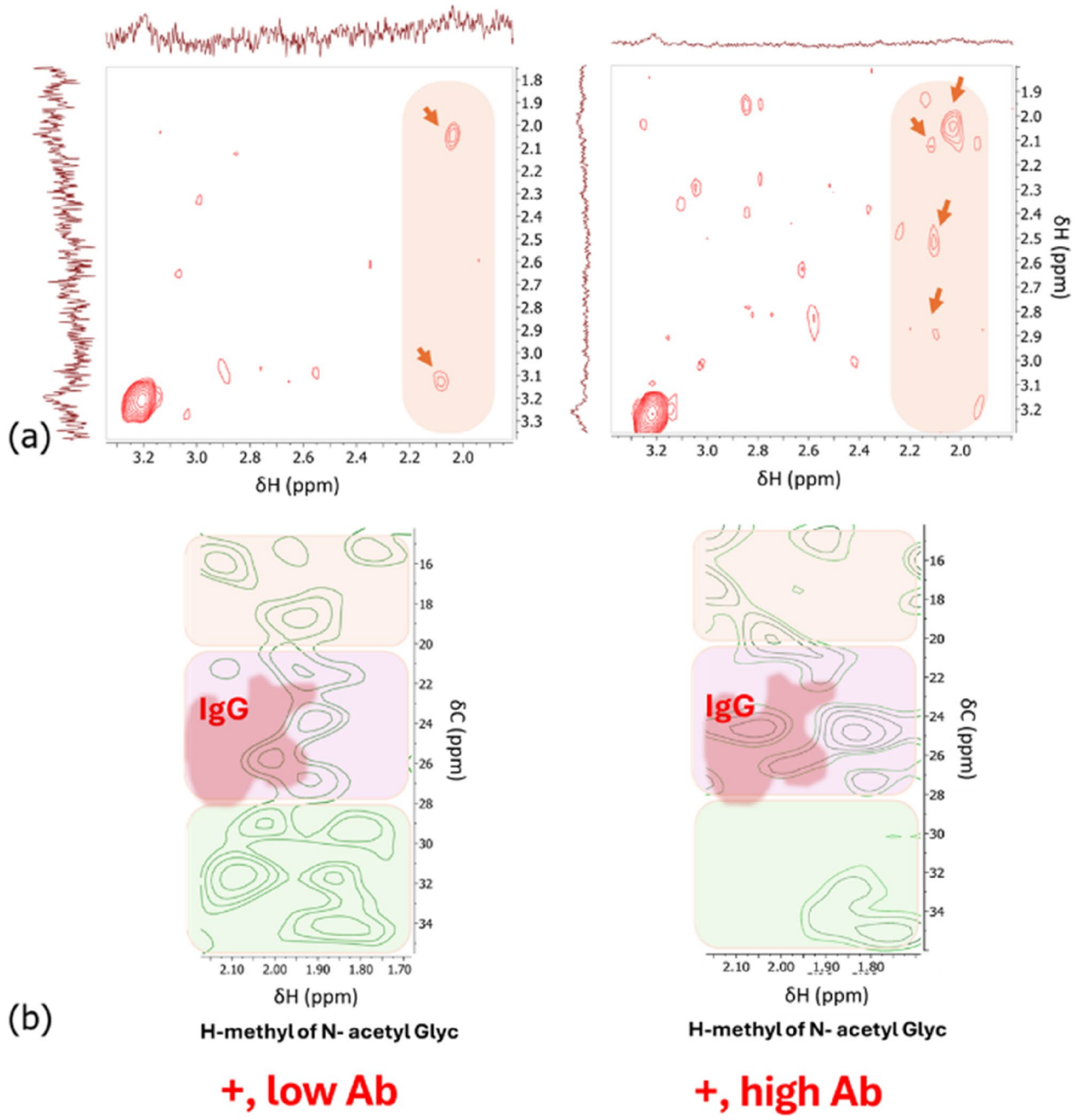


Fig. 3 **a** Detail of GLYC zone for ^{1}H-^{1}H COSY to profile Leishmania-positive sera with low Ab content and Leishmania-positive sera with high Ab content; **b** Detail of GLYC zone for ^{1}H:^{13}C HSQC to profile Leishmania-positive sera with low Ab content and Leishmania-positive sera with high Ab content. Orange ^{13}C zone: signals of protein methionine ε-methyl groups (15–19 ppm); Pink ^{13}C zone: N-acetyl methyl groups of glycans GLYC (20–27 ppm); Green ^{13}C zone: lipidic allyl groups in yellow (27–35 ppm)

nature of this method offers encouraging predictive values in follow up and progression, towards differentiation of early diseased animals by the detection and quantification of CICs.

Post-translationally modified proteomes often contain proteins and peptides bearing specific bioorganic tags resulting from metabolic modifications (e.g., phosphorylation, cysteine oxidation, ubiquitin flagging), as well as aliphatic modifications (e.g., methylation, large acylation, low molecular acetylation and glycosylation) [19]. Beyond the opportunity of profiling the proteins modifications linked to aging [20], cancer [21] and dysmetabolism [22], only a few studies have reported the detection of circulating modified proteins in parasitic

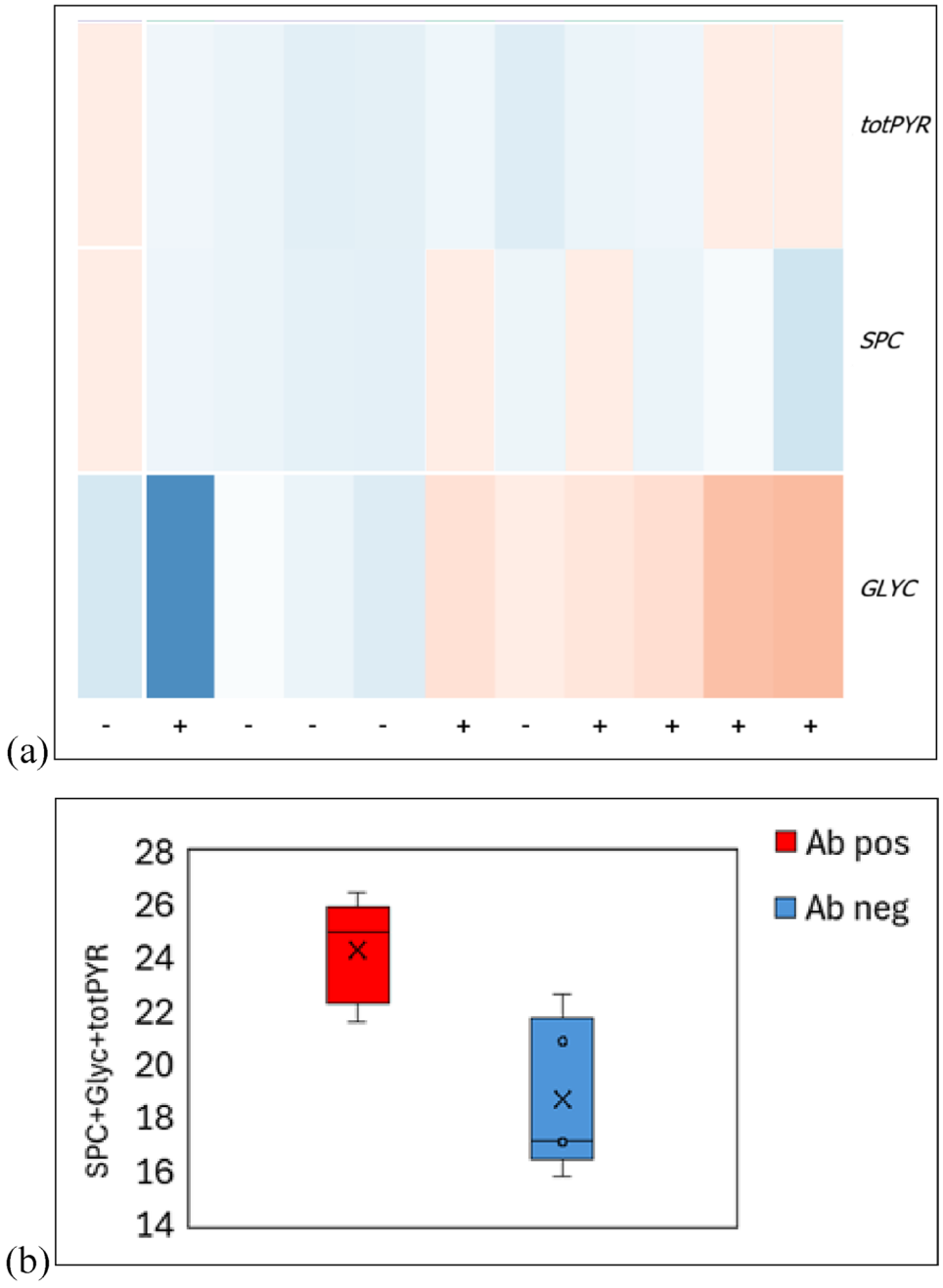


Fig. 4 **a** Statistical mapping and correlative analyses exploiting 3 variable 1D-NMR integrative buckets: distinction of Ab^+ vs Ab^- *Leishmania* positive sera; **b** box-histograms distribution of cumulative data (*Total*^{1}*H Signals*) for SPC, GLYC and total PYR zones (early and late, considered under the same integration bucket

diseases using liquid chromatography/mass spectrometry or immunochemistry techniques [23, 24]. Monitoring pure organic traces within proteomes through structural spectroscopy, such as NMR, to correlate chemical profiles with physiological versus pathological states in parasitic infection remains a significant challenge. Therefore, leishmaniosis represents an ideal immune-mediated pathological model for applying relative quantification of antibodies (e.g., glycosylated proteins) in biological sera. Importantly, zoonotic CanL caused by *L. infantum*, has the domestic dog as the main reservoir, [24] with potentially lethal outcomes. Its pathogenesis in the canine host is driven by two interconnected cascades represented by (i) pro-inflammatory response, involving a rise in general inflammatory glycoproteins and (ii) formation of soluble CICs, with a marked increase in circulating antibodies, deposition in capillary walls, resulting in multi-organ syndrome. The progressive elevation of sCIC

concentration ultimately contributes to organ dysfunction, coagulopathies and fatal systemic failure [10].

Modified sugar-related signals in mammalian sera have become a central focus of non-invasive spectroscopic investigations aimed at rapidly distinguish diseases from healthy individuals. In the present study, low-field benchtop NMR technology was employed to discriminate between *Leishmania*-positive from negative-dogs. The initial one-dimensional low field NMR analysis targeted three key bioorganic traces (i.e., GLYC, SPC and PYR areas) associated with serum modifications. Simple statistical correlations demonstrated that the *Leishmania*-positive cohort could be effectively separated from negative controls. Furthermore, within the positive cohort, the analysis discriminated samples characterized by high levels of circulating antibodies and immune complexes vs. those with low antibody titers. This refined discrimination was achieved by incorporating additional bucket areas within the PYR chemical traces and by performing detailed two-dimensional NMR analyses, moving from proton-proton to proton-carbon profiles. Notably, late and early PYR signals were strongly associated with cyclic ring -CH structures of different branched sugars, from different stages of protein glycosylation. This area reflects the sequential attachment and maturation of oligosaccharide chains, hence, discriminating signals from immature or mature glycans, may differentiate physiological or pathological processes (e.g., acute inflammatory activation and cellular stress from chronic metabolic alterations). Importantly, the overall increase of PYR signals observed in sera with high antibodies concentration can be explained by the conserved glycan core motif G-M-GNac (Glucose, Mannose, N-acetylglucosamine), which anchors to the protein core of these immunological proteins. In particular, the organic ring of mannose residues within the trimeric moiety contributes strongly to the entire PYR region (Figure S5, Table S3), explaining the pronounced PYR peaks observed in high antibody sera [25].

A possible physio-pathological explanation lies in the maturation and secretion dynamics of glycoproteins. Infection stimulates both the endoplasmic reticulum and the Golgi apparatus to produce N-glycosylated IgG, always starting from the G-M-GNac moiety. Although mature IgGs do not directly contribute to the EARLY-PYR signal, their massive systemic production inevitably reflects in increased protein synthesis and subsequent post-translational modifications. This mechanism accounts for the observed increase in circulating early-stage glycosylated proteins, which are considered markers of protein synthesis activity and acute secretion. Consequently, the detection of early glycosylated NMR signals in serum is indicative of an active inflammatory response, reflecting the accelerated protein production and trafficking triggered by the immune response.

To date, variations in the glycobiome have been studied by evaluating fucose residues [26], the degree of terminal sialylation and N- and O-branching or linking of sugars [27], and variations in acetylation status [28] predominantly through classical biochemical tools and electromagnetic inputs. Within the context of infectious diseases, NMR applications remain limited, with only two notable examples concerning HIV [29] and tripanosomiasis [30]. Importantly, the distinction between the current study and the latter two, lies in the nature of the biomarkers investigated. Indeed, previous studies focused on metabolic indicators indirectly associated with systemic dysregulation, whereas the present study demonstrated a direct correlation between specific bioorganic signals and pathological status. Here, spectral traces reflected (i) oxidative stress associated with cellular response on parasitic infection, and (ii) glycoacetyls of antibodies in activated immune states, which are directly correlated with a pathological state due to circulating immune complexes. Further longitudinal studies are needed to assess the predictive value of the NMR method in distinguishing early diseased animals, from infected yet asymptomatic ones.

Conclusion

Overall results demonstrated that benchtop methods, characterized by rapid acquisition times, minimal invasiveness, and negligible sample preparation, offer a suitable analytical approach for preclinical applications and underscore the potential of advanced chemical profiling tools for clinically relevant outcomes. Specifically, this study expands the scope of glycometabolic profilometry using a novel chemical-based approach to evaluate clinical and predictive markers in immune-mediated parasitic diseases. NMR was herein demonstrated to be useful in detecting sudden increases in circulating antibodies and immune complexes, events that predispose the hosts to systemic dysregulation and disease. Future studies are pivotal to assess the predictive value of this application in identifying early-stage systemic immune dysregulation associated with the Th2 humoral non protective response, with ultimately ends in sCIC deposition and progression of CanL, paving the way to the potential prediction of this (and other similar) illness state progression and follow up.

Supplementary Information

The online version contains supplementary material available at https://doi.org/10.1186/s12575-026-00328-2.

Supplementary Material 1. Table S1: Investigation ranged areas for 1D-1H-NMR of canine blood sera, organized in buckets (b1-b12) [31].

Acknowledgements
I acknowledge dr. Ruth Boetzel and dr. Nicola Di Masi for scientific exchange about the review answer process.

Authors' Contributions
J.M.R., P.A.: formal analysis, validation, supervision, writing. C.D., M.A., M.C., M.V., M.D.: formal analysis, validation. M.S., D.O., M.D.A.: validation, supervision, funding. D.V.: Experimental design, investigation, methodology, supervision, writing.

Funding
This research was funded under the National Recovery and Resilience Plan (NRRP), Mission 4-'Education and Research', Component 2-'From Research to Business', Investment 1.4-'Strengthening research structures and creating R&D' national champions 'on specific key enabling technologies (Agritech)', CUP: H93C22000440007, code: CN_00000022, and by OnFoods, Project code PE00000003, Concession Decree No. 1550 of 11 October 2022 adopted by the Italian Ministry of University and Research, CUP H93C22000630001, Project title 'ON Foods – Research and innovation network on food and nutrition Sustainability, Safety and Security – Working ON Foods'. This work was partially supported by EU funding within the Next Generation EU-MUR PNRR Extended Partnership initiative on Emerging Infectious Diseases (Project no. PE00000007, INF-ACT).

Data Availability
The accessory data presented in the study are included in Supporting Information Section.

Declarations

Ethics Approval and Consent to Participate
Protocols for collection of dog samples were approved by the ethical committee of the Department of Veterinary Medicine of the University of Bari, Italy (Prot. Uniba 12/20).

Competing Interests
The authors declare no competing interests.

Received: 22 December 2025 / Accepted: 6 February 2026
Published online: 13 February 2026

References

1. Alonso-Moreno P, Rodriguez I, Izquierdo-Garcia JL. Benchtop NMR-Based metabolomics: first steps for biomedical application. Metabolites. 2023;13:614.
2. Wist J, et al. Benchtop proton NMR spectroscopy for High-Throughput lipoprotein quantification in human serum and plasma. Anal Chem. 2025;97:6399–409.
3. Lodge S, et al. NMR Spectroscopy-Based lipoprotein and glycoprotein biomarkers differentiate acute and chronic inflammation in diverse healthy and disease population cohorts. J Proteome Res. 2025;24:4191–201.
4. Mallagaray A, et al. Towards a precise NMR quantification of acute phase inflammation proteins from human serum. Angew Chem. 2023;135:e202306154.
5. Muhlestein JB. Both the novel, NMR biomarker of inflammation glyca, and, hs-crp are independent, and additive predictors of future cardiovascular events among patients undergoing coronary angiography: results from the intermountain heart collaborative study. J Am Coll Cardiol. 2017;69:1069.
6. Vacca M, et al. Cholesterol-Lowering and radical scavenging potential of fermented black Kale (Brassica Oleracea var. acephala): from Pilot-Scale production to in vivo study. ChemFoodChem. 2025;e00035. https://doi.org/10.1002/cfch.202500035.
7. Levine JA, et al. Associations of glyca and high-sensitivity C-reactive protein with measures of lipolysis in adults with obesity. J Clin Lipidol. 2020;14:667–74.
8. Nitschke P, et al. Direct low field J-edited diffusional proton NMR spectroscopic measurement of COVID-19 inflammatory biomarkers in human serum. Analyst. 2022;147:4213–21.
9. Mendoza-Roldan J, et al. Leishmania infantum and dirofilaria immitis infections in Italy, 2009–2019: changing distribution patterns. Parasites Vectors. 2020;13:193.
10. Gernone F, et al. Canine leishmaniosis and peripheral neuropathy: a lesson from the neurologist. Parasites Vectors. 2025;18:222.
11. Sarquis J, et al. Clinical validation of Circulating immune complexes for use as a diagnostic marker of canine leishmaniosis. Front Vet Sci. 2024;11:1368929.
12. Behrens A-J, et al. Glycosylation profiling of dog serum reveals differences compared to human serum. Glycobiology. 2018;28:825–31.
13. Mendoza-Roldan JA, et al. Detection of leishmania tarentolae in lizards, sand flies and dogs in Southern Italy, where leishmania infantum is endemic: hindrances and opportunities. Parasites Vectors. 2021;14:461.
14. Otranto D, et al. Toward diagnosing *Leishmania infantum* infection in asymptomatic dogs in an area where leishmaniasis is endemic. Clin Vaccine Immunol. 2009;16:337–43.
15. Francino O, et al. Advantages of real-time PCR assay for diagnosis and monitoring of canine leishmaniosis. Vet Parasitol. 2006;137:214–21.
16. Maebayashi M, Ohba M, Takeuchi T. Anomeric proportions of d -glucopyranose at the equilibrium determined from 1 H-NMR spectra I. Investigation of experimental conditions and concentration dependence at 25.0°C. J Mol Liq. 2017;232:408–15.
17. Pang Z, et al. MetaboAnalyst 6.0: towards a unified platform for metabolomics data processing, analysis and interpretation. Nucleic Acids Res. 2024;52:W398–406.
18. Nitschke P, et al. J-Edited diffusional proton nuclear magnetic resonance spectroscopic measurement of glycoprotein and supramolecular phospholipid biomarkers of inflammation in human serum. Anal Chem. 2022;94:1333–41.
19. Dunphy K, Dowling P, Bazou D, O'Gorman P. Current methods of Post-Translational modification analysis and their applications in blood cancers. Cancers. 2021;13:1930.
20. Vanhooren V, Laroy W, Libert C, Chen C. N-Glycan profiling in the study of human aging. Biogerontology. 2008;9:351–6.
21. Geffen Y, et al. Pan-cancer analysis of post-translational modifications reveals shared patterns of protein regulation. Cell. 2023;186:3945–e396726.
22. Duchovni L, Shmunis G, Lobel L. Posttranslational modifications: an emerging functional layer of diet-host-microbe interactions. mBio. 2024;15:e02387–24.
23. Prisco F, et al. Leishmania spp.-Infected Dogs Have Circulating Anti-Skeletal Muscle Autoantibodies Recognizing SERCA1. Pathogens. 2021;10:463.
24. Agallou M, Athanasiou E, Samiotaki M, Panayotou G, Karagouni E. Identification of immunoreactive leishmania infantum protein antigens to asymptomatic dog Sera through combined immunoproteomics and bioinformatics analysis. PLoS ONE. 2016;11:e0149894.
25. He M, Zhou X, Wang X. Glycosylation: mechanisms, biological functions and clinical implications. Sig Transduct Target Ther. 2024;9:194.
26. Mondal G, Chatterjee U, Das HR, Chatterjee BP. Enhanced expression of α1-acid glycoprotein and fucosylation in hepatitis B patients provides an insight into pathogenesis. Glycoconj J. 2009;26:1225–34.
27. Mondal G, Chatterjee U, Chawla YK, Chatterjee BP. Alterations of glycan branching and differential expression of Sialic acid on alpha Fetoprotein among hepatitis patients. Glycoconj J. 2011;28:1–9.
28. Kissel T, Toes REM, Huizinga TWJ, Wuhrer M. Glycobiology of rheumatic diseases. Nat Rev Rheumatol. 2023;19:28–43. https://www.nature.com/articles/s41584-022-00867-4.
29. Tibuakuu M, et al. GlycA, a novel inflammatory marker, is associated with subclinical coronary disease. AIDS. 2019;33:547–57.
30. Lamour SD, et al. Discovery of infection associated metabolic markers in human African trypanosomiasis. PLoS Negl Trop Dis. 2015;9:e0004200.
31. Rosqvist F, et al. Circulating fatty acids from high-throughput metabolomics platforms as potential biomarkers of dietary fatty acids. Clin Nutr. 2022;41:2637–43.

Publisher's Note

Springer Nature remains neutral with regard to jurisdictional claims in published maps and institutional affiliations.

Supporting Information

Leishmania infection: a bioorganic model under the *light* of benchtop low field Nuclear Magnetic Resonance

---

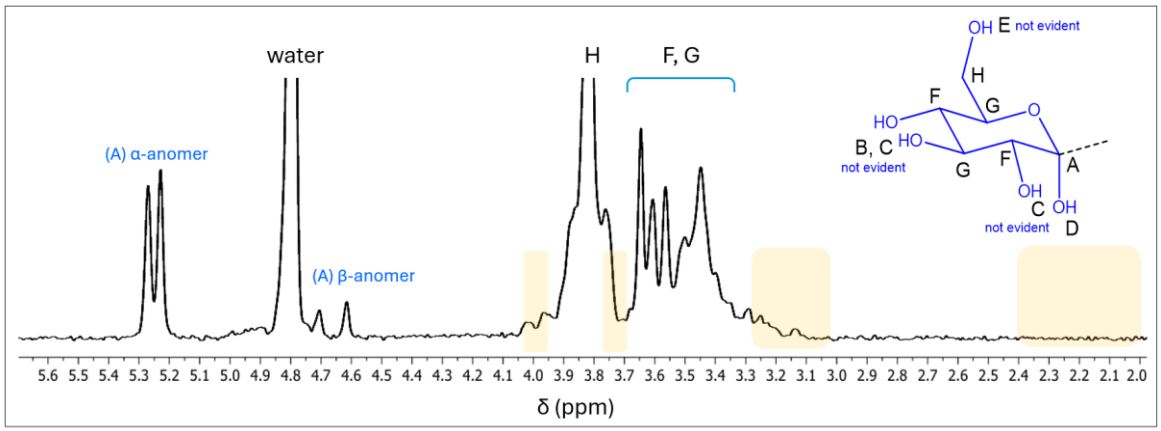
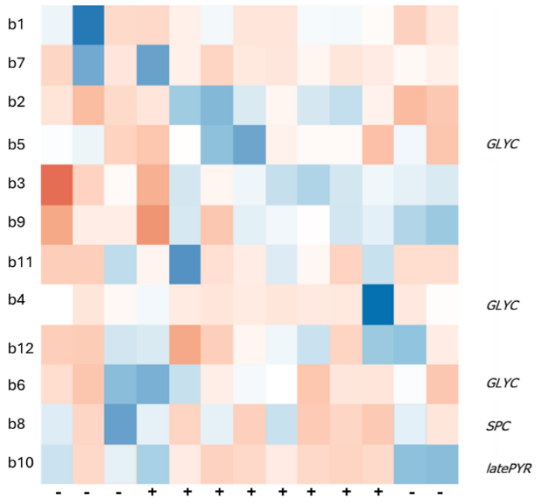


Figure S1| ^{1}H NMR spectrum and Chemical shift peaks attribution to D-(+)-glucose in water solution. Yellow areas: non-overlapping investigated zones.

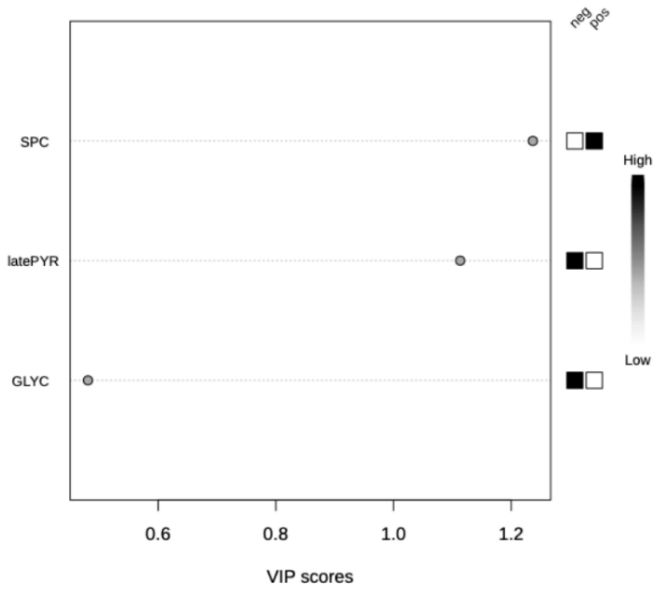
	δ,ppm	**Chemical attribution**
b12	δ: 5.92 - 5.60	alkenyl from unsaturated fatty acids[31], pyranose
b11	5.46 - 5.12	alkenyl from unsaturated fatty acids, pyranose
b10	4.30 - 3.86	HC-anomeric, cy(ring)pyranose, late PYR
b9	3.86 - 3.46	cy(ring)pyranose, early PYR
b8	3.31 - 3.06	H_3-C in choline of phospholipids, SPC
b7	2.91 - 2.57	H-C-X, protein backbone
b6	2.18 - 2.09	H_3C-C=O N-acetyl, GLYC

b5	2.11 - 1.98	H_3-C-C=O N-acetyl, O-acetyl, GLYC
b4	1.98 - 1.80	H_3C-C=O N-acetyl, O-acetyl GLYC
b3	1.57 - 1.39	H_3-C-CH=CH-, lipid signals
b2	1.39 - 1.04	H_3-C-CH_2-, lipoproteins
b1	1.05 - 0.63 ppm	H_3-C-CH_2-, lipoproteins, H_3-C-alanin

Table S1. Investigation ranged areas for 1D-^{1}H-NMR of canine blood sera, organized in buckets (b1-b12).



(a)



(b)

Figure S2|(a) Statistical mapping and correlative analyses exploiting 12 bucket areas or variable 1D-NMR integrative buckets: distinction of negative vs positive sera.(b) VIP plot exploited to define VIP scores for Leishmania + vs – discrimination.

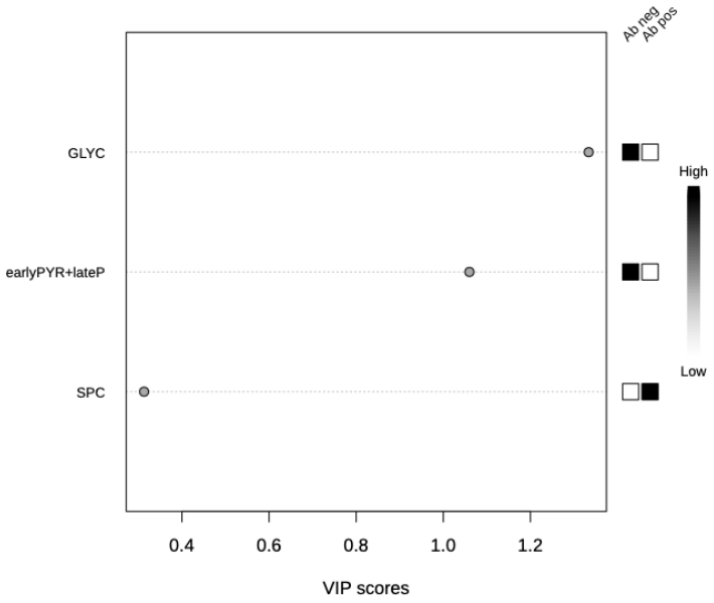
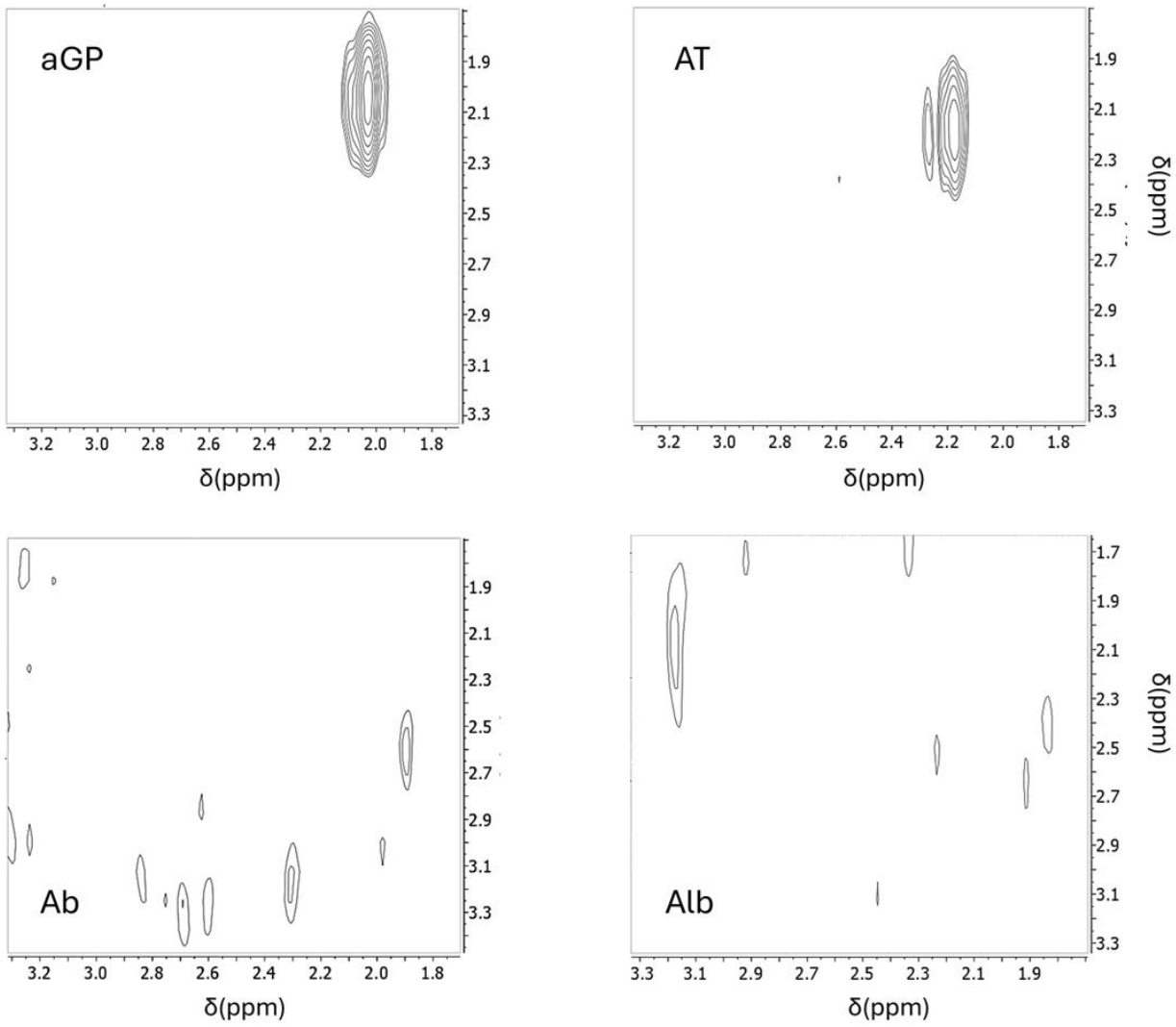


Figure S3|VIP plot exploited to define VIP scores for Leishmania + (AB+) vs (AB-).

Sample	**δ,ppm (H)1D, Glyc attribution**
α1-acid glycoprotein purified from plasma (GP)	2.05
α1-acid glycoprotein purified from plasma, cow (GPc)	2.18-2.11
α1-antitrypsin purified from plasma (AT)	2.23- 2.19
dog antibody purified from plasma (Ab), weak glyc. signals	2.45

macromolecular Ab complex from pig (mAb), high glyc. signal	1.89-1.49
albumin protein (Alb)	-

Table S2. GLYC ^{1}H-NMR signals for standard macromolecules.



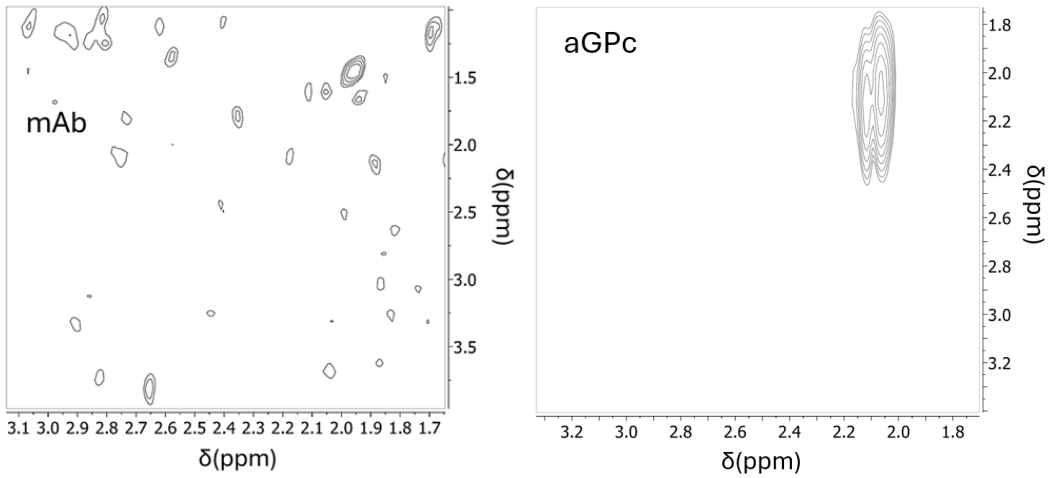
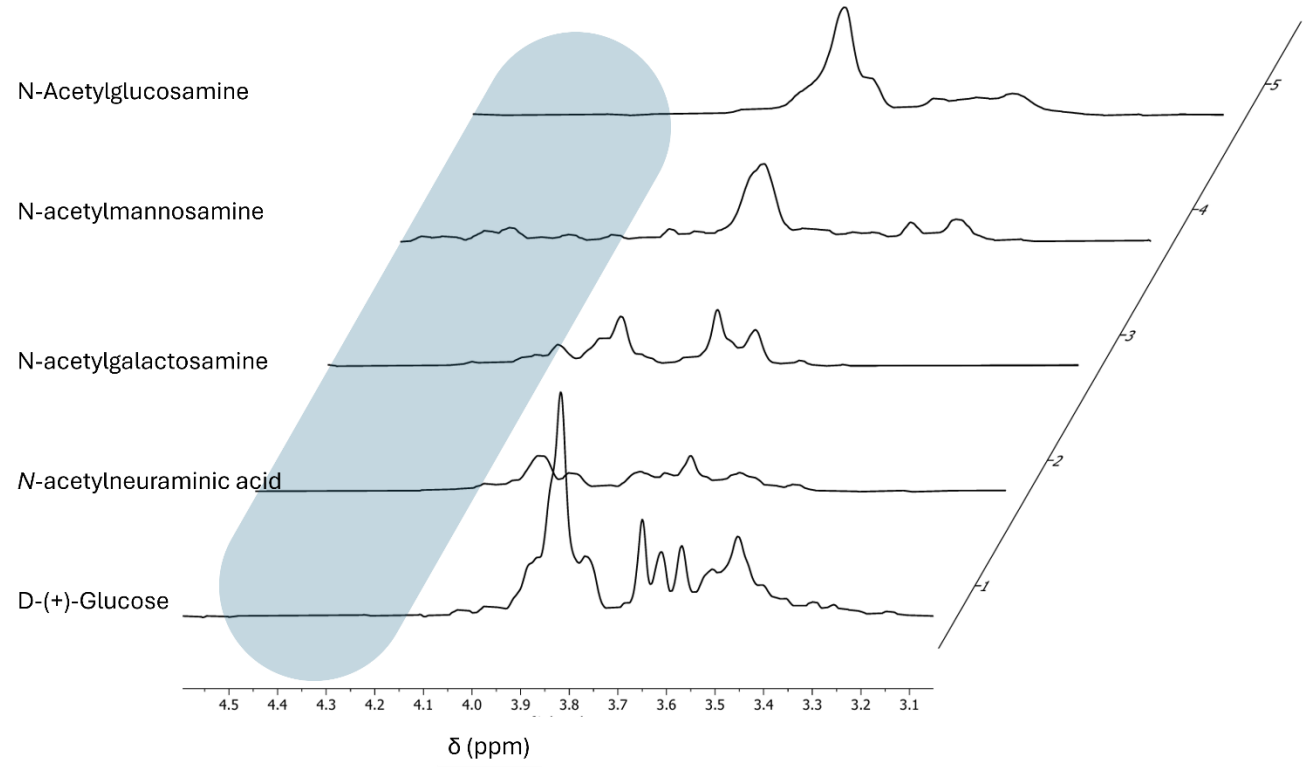
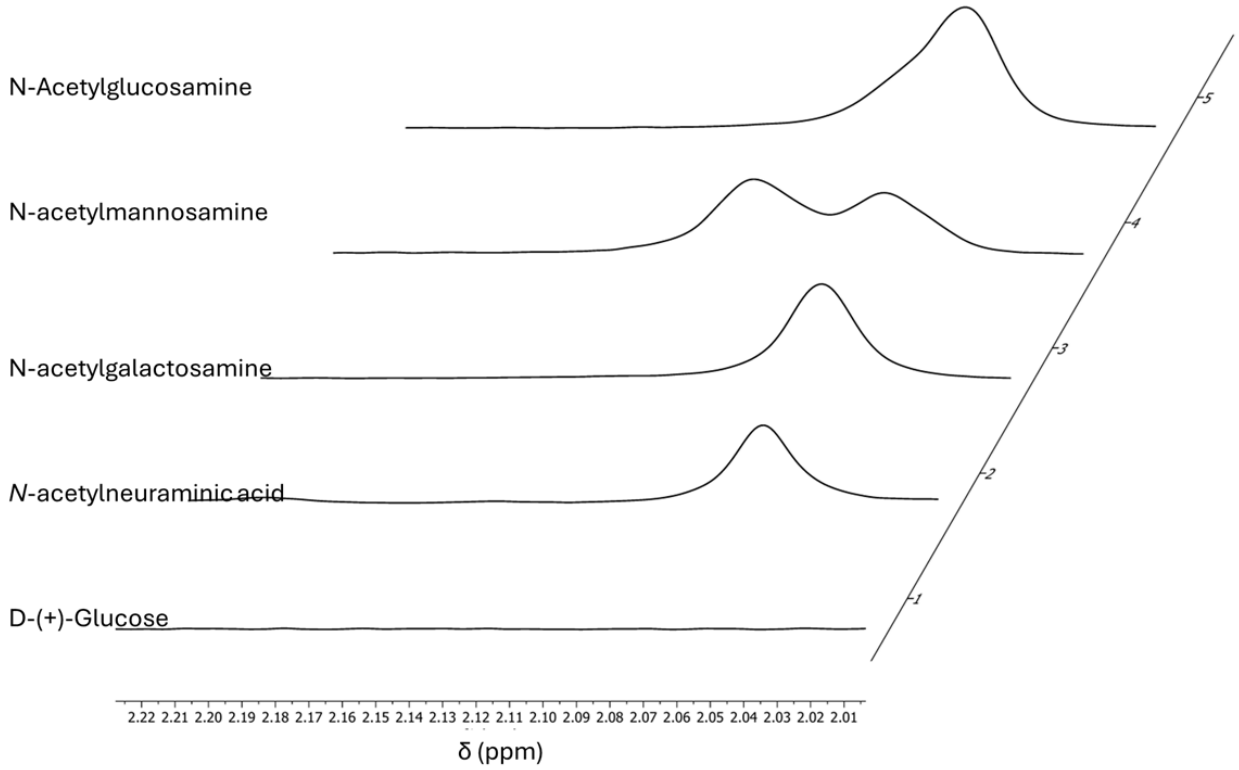


Figure S4| Detail of GLYC zone for ^{1}H-^{1}H COSY to profile glyco- and non-glycoprotein standard biomolecules: α1-acid glycoprotein purified from plasma (GP), cow α1-acid glycoprotein purified from plasma (GP), α1-antitrypsin purified from plasma (AT), dog antibody (Ab) purified from plasma (Ab, low glycosylation state), albumin protein (Alb), macromolecular Ab complex from pig (mAb, high glycosylation state).



(a)



(b)

Figure S5| ^{1}H NMR spectrum of sugar standard molecules recorded in water solution (a, Pyr zone; b, Glyc zone).

Sample	**δ,ppm (H)1D, Glyc attribution**
D-(+)-Glucose	-
N-acetylneuraminic acid	2.07
N-acetylgalactosamine	2.08
N-acetylmannosamine	2.12, 2.07
N-acetylglucosamine	2.09

Table S3. Investigation ranged Glyc areas for ^{1}H NMR for sugar standard molecules.